

Exchange grant final report

Title

Development of a new method for mapping the sensitivity of plasmonic nanostructures for biosensor applications

Duration

3 weeks starting September 9, 2010

Applicant

Marek Piliarik, Ph. D.
Institute of Photonics and Electronics (IPE)
Chaberska 57
18251 Prague
Czech Republic

Receiving institution

Institute of Physics
Karl-Franzens-University Graz (KFU)
Universitätsplatz 5
A-8010 Graz, Austria

Introduction

Merging the capabilities of novel photonic nanostructures and biosensors applications is in the forefront of nanobiophotonic research. Biosensors based on surface plasmon resonance (SPR) represent an established technology for analysis of biomolecular interactions and detection of numerous important biomolecular analytes [1], including DNAs [2, 3], antibodies, protein biomarkers [4], and small organic compounds [5]. Localized surface plasmons (LSPR) on metallic nanoparticles were proved to provide higher confinement of electromagnetic field comparing to propagating surface plasmons. Higher field localization can result in higher sensitivity to biomolecular binding events taking place at certain areas of the nanoparticle surface. Therefore targeting biomolecular interactions to areas with increased sensitivity can potentially improve the performance of SPR biosensors [6]. However, there are only very few reports suggesting that the performance of LSPR based biosensors is competitive to propagating SPR based biosensors [7]. Research on LSPR based biosensors to date

lacks experimental data allowing for comparison of their performance with the state-of-the-art in biosensors based on propagating SPR.

In this project a new experimental method was utilized to characterize the spatial distribution of the LSPR sensitivity. The geometry of arrays of nanoparticles was optimized for biosensor applications and a model detection experiment was carried out allowing for direct comparison of the optimized LSPR based biosensor with an established SPR biosensor technology.

Purpose of the visit

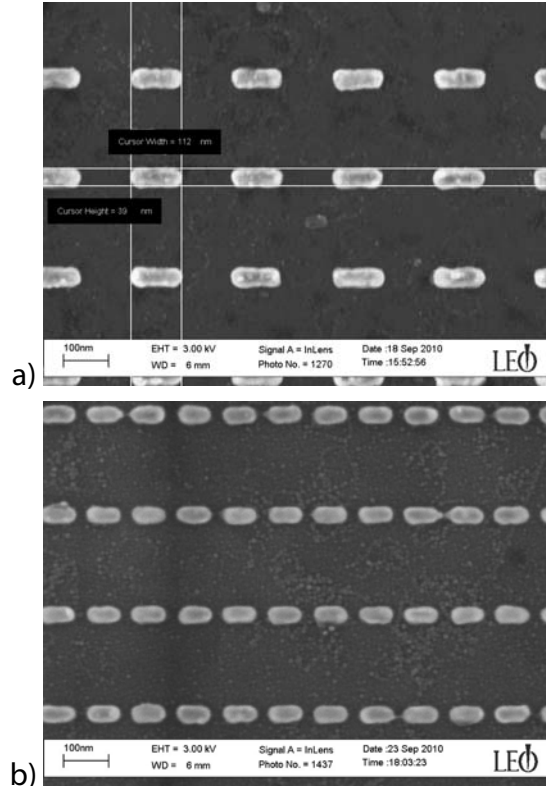
The aim of the project was to combine 2-dimensional metallic nanoparticle arrays with biomolecular assays and characterize the sensitivity of LSPR structures to local changes of refractive index (e.g. induced by biomolecular interaction). The optimization of the geometry of nanoparticle arrays for biosensor application was carried out based on previous performance analysis of biosensors based on propagating SPR [8]. Arrays of metallic nanoparticles were fabricated using electron beam lithography during the visit at the receiving institution. Tested nanostructures included arrays of nanorods, nanoantennas, and nanorod chains. Developed nanoparticles were characterized with electron microscopy and microspectrometry. The distribution of sensitivity in the proximity of developed nanoparticles was analyzed experimentally using a polymer mask prepared on top of the nanostructure. Two-step lithography procedure was employed for the experimental characterization during the stay. Resulting nanoparticle arrays were combined with biomolecular assay optimized using conventional SPR technology at the Institute of Photonics and Electronics (IPE). Hybridization of short DNA strands was employed as a model system triggering the change of refractive index in the vicinity of nanoparticles.

Experimental

Nanoparticles fabrication (carried out at KFU)

Gold nanoparticles were fabricated on indium-tin-oxide (ITO) covered glass substrates by electron beam lithography using a positive resist poly(methyl methacrylate) (PMMA). PMMA layer was developed and substrates were coated with 30 nm gold layer by means of thermal evaporation (0.5 nm chromium layer was used as an adhesion promoting layer). Nanoparticle array preparation was finished by the lift-off in acetone.

Developed nanoparticle arrays were characterized with electron microscopy and transmission spectra were measured with conventional optical microscope connected to a spectrometer (microspectrometry). The thickness of the gold layer was measured using profilometry. Three types of nanoparticle arrays were investigated in this project: array of separated *nanorods*, array of *nanorod chains* and array of *antennas* as illustrated in Figure 1 a), b), and c) respectively. Nanoparticle arrays were investigated in terms of the reproducibility of its transmission spectra measured at different positions of the nanoparticle arrays (spot size $\sim 10 \mu\text{m}$). An example of the transmission spectra variation is presented in Figure 2a for the array of nanorods and in Figure 2b for the array of nanorod chains. Figure 2 indicates that the resonant wavelength variation is less than 10 nm and the spot-to-spot variation in the width of transmission spectra is less than 15 nm for both nanoparticle structures.



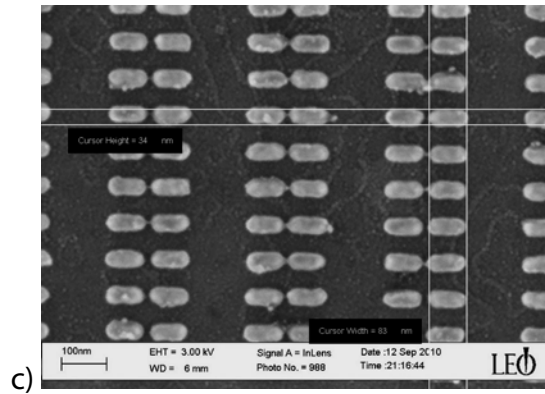
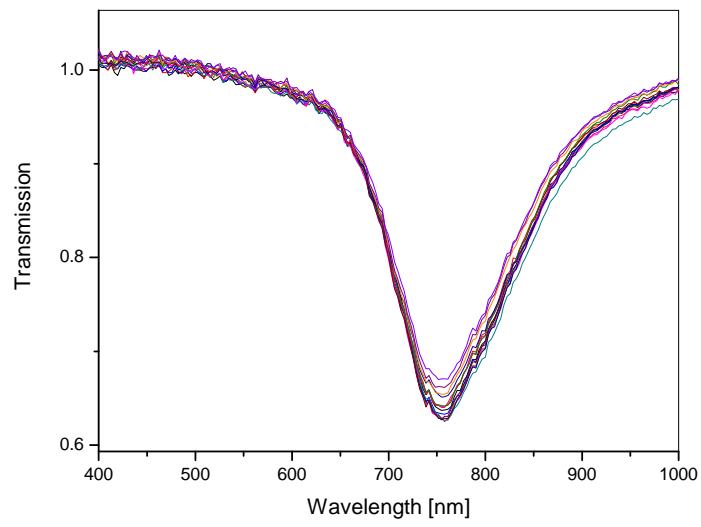
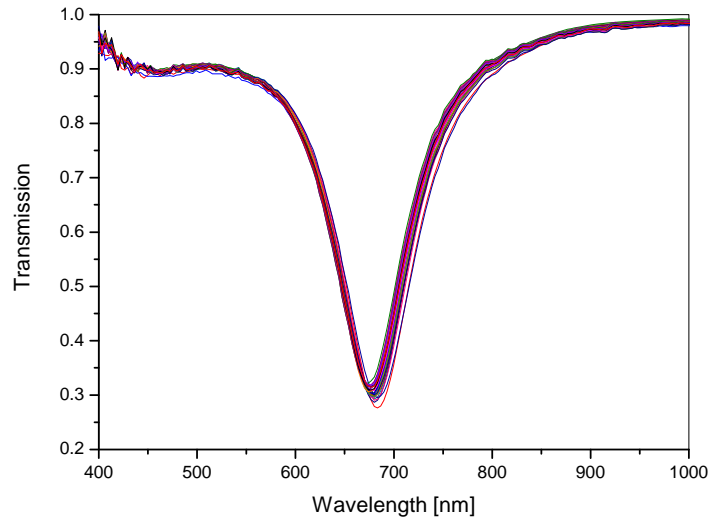


Figure 1 Examples of fabricated nanostructures (SEM images). a) Array of nanoparticles (110 nm × 40 nm, periodicity 250 nm × 250 nm). b) Array of nanoparticle chains (80 nm × 40 nm, periodicity 100 nm × 220 nm). c) Array of nano-antennas (180 nm × 35 nm, 15 nm gap, periodicity 80 nm × 300 nm).



a)

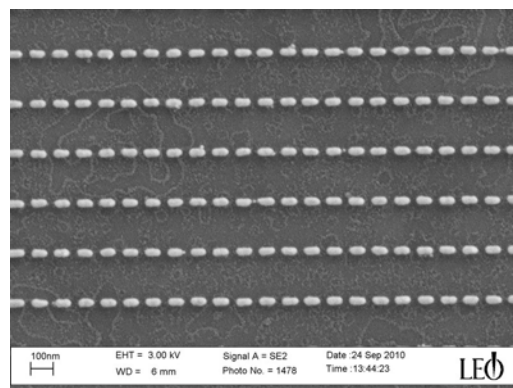


b)

Figure 2 Transmission spectra of (a) the array of separated nanorods and (b) the array of nanorod chains measured at 30 different positions of a $150\ \mu\text{m} \times 150\ \mu\text{m}$ area.

Nanoparticle array masking (carried out at KFU)

The distribution of sensitivity in the proximity of developed nanoparticles was analyzed experimentally using e-beam lithography of a second PMMA layer serving as a mask prepared on top of the nanostructure. Two-step lithography procedure was carried out on substrates comprising an array of nanorod chains. 60 nm thick PMMA layer was used to mask the nanoparticle array and second lithography step aligned with the first lithography layer was used to unmask designated areas of the array. The alignment precision was found to be better than 10 nm. The success rate in the second layer mask targeting either the nanorod position or the gap between the nanorods was better than 80%. Figure 3 compares an array of nanorod chains with the result of the second step lithography mask.



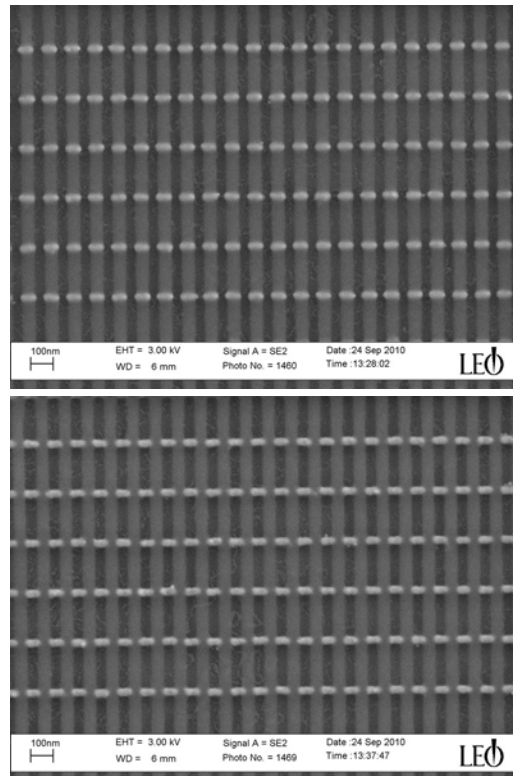


Figure 3 SEM images of the array of a) nanorod chains without the secondary lithography mask, b) with the mask across the centers of nanorods, and c) with the mask across the gaps between nanorods.

Microfluidics (carried out at KFU)

In order to carry out the microspectrometry of nanoparticle structures in liquid environment, simple microfluidics was developed. The substrate was interfaced with a flow-cell facing the nanoparticle array. Flow chamber was formed from 60- μm -thick self-adhesive vinyl foil which was attached to the surface of a transparent acrylic cover slide, Figure 4. Syringe pump was used to deliver liquid sample to the investigated nanoparticle array.

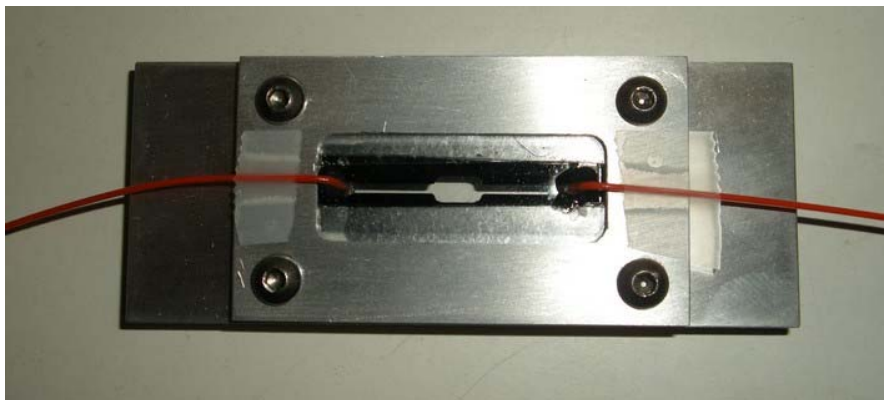


Figure 4 Photograph of the microfluidics developed for the transmission microspectrometry and characterization of nanoparticle arrays.

Multichannel ATR spectroscopy (carried out at IPE)

A laboratory SPR biosensor developed at IPE is based on wavelength spectroscopy of surface plasmons utilizing attenuated total reflection method (ATR) [9] and allows for monitoring biomolecular interactions in four independent sensing channels. For the real-time spectroscopy of localized surface plasmons, sensor chip comprising nanoparticle arrays in two or four sensing areas ($0.6 \text{ mm} \times 1 \text{ mm}$) was interfaced with the base of the ATR prism. White light from a halogen light was collimated and made incident through the prism on the sensing areas. The reflected light was collected using graded index lenses into four optical fibers and guided to a multichannel spectrometer (Ocean Optics, USA). The sensor chip was interfaced with a flow-cell with four separate flow chambers facing four sensing areas on the sensor chip. The gasket forming flow chambers (60- μm -thick vinyl foil) was attached to the surface of a polished acrylic manifold. The flow chambers were designed to provide a laminar flow along the sensor surface. The volume of each flow chamber was about $0.2 \text{ }\mu\text{L}$. A multichannel peristaltic pump was used to flow liquid samples over each sensing channel.

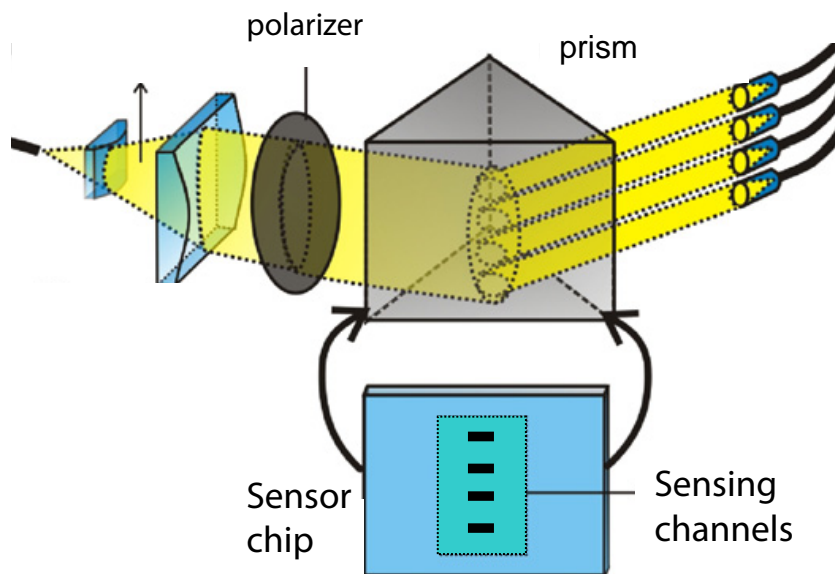


Figure 5 Scheme of four channel SPR sensor based on spectroscopy of surface plasmons in ATR configuration.

Nanoparticle functionalization (carried out at IPE)

The functionalization of nanoparticles with thiolated DNA oligonucleotides was optimized for maximum surface concentration of DNA probes immobilized on the nanoparticle surface. Similar optimization was previously carried out with biosensor based on propagating SPR [10]. The functionalization of nanoparticle arrays and LSPR based detection experiments were in parallel carried out with propagating SPR for reference.

The thiolated DNA oligonucleotide SdT20 SH-5'-dT20-3' was used as a capture probe for dA20 (5'-dA20-3') detection. SPR chips were functionalized by attaching the thiol-derivatized DNA probes to the gold surface. 1 μM solution of thiolated DNA probes in TrisMg buffer (10 mM Tris-HCl, 30 mM MgCl₂) was injected at a flow rate of 5 $\mu\text{L}/\text{min}$ for 40 minutes. Both the measuring and reference sensor surface were incubated in 200 mM blocking alkanethiol solution (HS-(CH₂)₆-OH; Sigma Aldrich, USA). PBS buffer was injected at 30 $\mu\text{L}/\text{min}$ for 5 minutes, followed by 5 mM NaOH for 5 minutes and finally washed with PBS.

Detection of oligonucleotides (carried out at IPE)

First, the running buffer (10 mM Tris-HCl, 15 mM MgCl₂, pH 7.4 at 25°C) was introduced until a stable baseline was established. Then, the solution of dA20 oligonucleotide in the running buffer was injected and flowed through the flow-cell for 5 minutes. The sensor surface was flushed with buffer for 5 minutes. Experiment based on propagating SPR allowed for surface regeneration with 2-minute injection of 20 mM sodium hydroxide. To compensate for changes in refractive index and the non-specific adsorption, the measurements were performed simultaneously in the sensing channel and reference channels and the response in the reference channel was subtracted from that in the sensing channel.

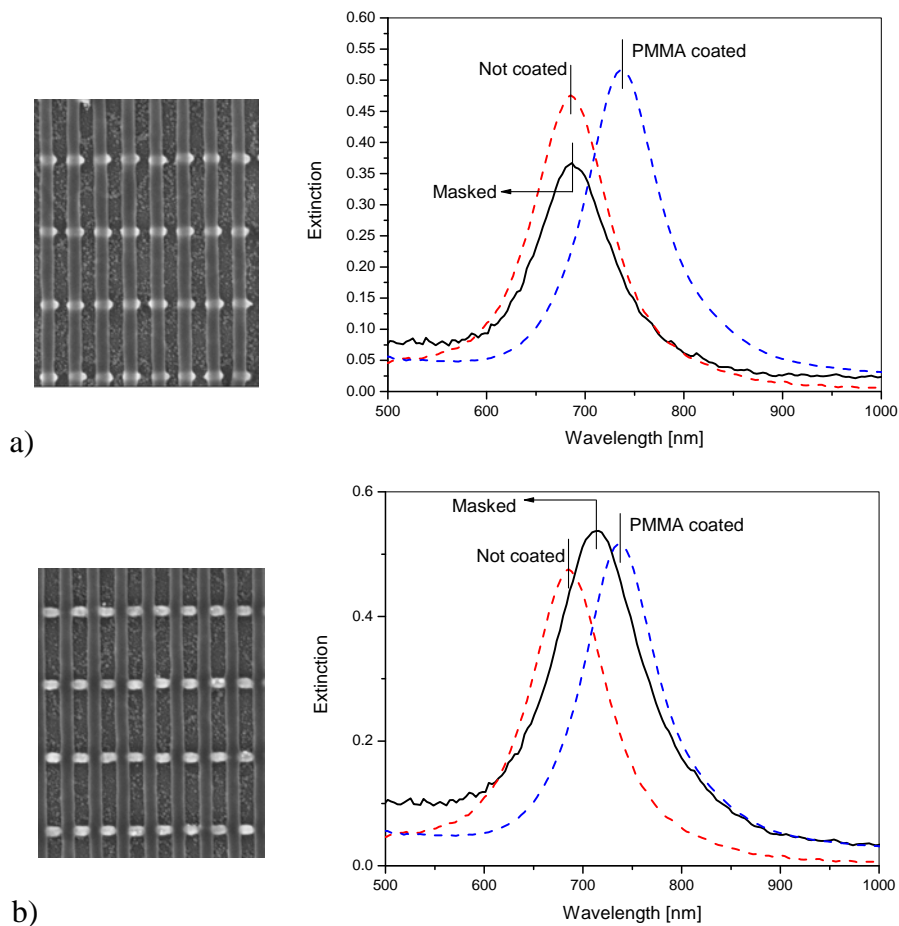
Results

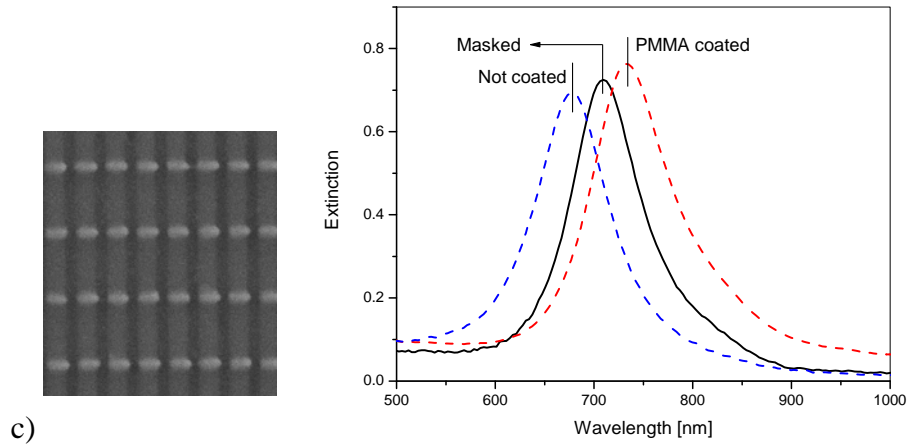
Mapping the sensitivity of nanoparticles

Figure 6 compares the extinction spectra corresponding to masked nanorod arrays with the extinction spectra of uncoated array and PMMA coated array. In Figure 6a it is demonstrated that the secondary lithography mask localized in the centers of nanorods results in an extinction peak shift by less than 5 nm. On a contrary Figure 6b shows, that identical lithography mask deposited across the tips of nanorods, results in a shift by more than 30 nm which is more than 60% of the total shift due to PMMA coated array. This indicates that the sensitivity to refractive index change is localized mostly at the tips of nanorods. The same experiment was carried out with different

width of the lithography mask, Figure 6c. The profile, of local sensitivity to refractive index change was derived from the relative extinction peak shift due to variation of the polymer mask overlap with the nanoparticle. Figure 7 depicts the measured spatial distribution of the sensitivity to local refractive index change. In order to illustrate the correlation of the sensitivity distribution with the field profile of the nanoparticle mode, electric field profile was calculated using FDTD modeling software (Lumerical Solutions, Inc., Canada) and plotted for comparison, Figure 7.

This new method for investigating the sensitivity of nanoparticle arrays presents an important experimental achievement in the research on nanoplasmonic biosensors. Full length publication resulting from this exchange research project is therefore in preparation to be submitted within several weeks.





c) Figure 6 Extinction spectra corresponding to different positions of the secondary mask compared to the extinction spectrum of uncoated array of nanoparticles and the extinction spectrum of fully coated array of nanoparticles.. (a) The mask covers the centers part of nanorods; (b) the mask covers the the gaps between nanorods; and (c) the mask covers the whole nanorod area.

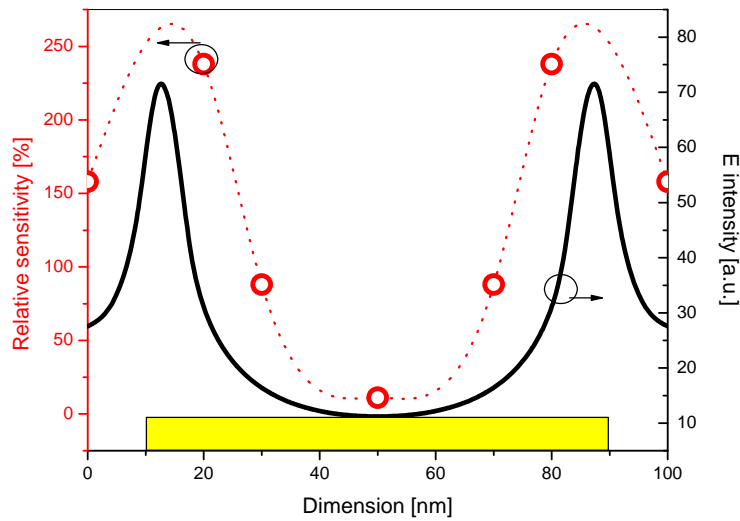


Figure 7 Measured profile of the local sensitivity (red circles) as a function of the position along the axis of the nanorod (one 100 nm period shown). Electric field profile calculated with FDTD is plotted for comparison (solid line).

Detection of oligonucleotides

In order to demonstrate the potential of developed nanostructures for biosensing and compare its detection capabilities with the performance of conventional SPR biosensors a model detection experiment was carried out. Hybridization of short DNA strands was employed as the model system. The same instrumentation,

functionalization protocol and assay were utilized in experiments based on SPR and LSPR spectroscopy. Figure 8 depicts the temporal sensor response (resonant wavelength shift) to the DNA hybridization taking place at the metallic surface for propagation SPR based biosensor and array of nanorods for LSPR based biosensor. Prior to the detection, a stable baseline in the running buffer is established in both SPR and LSPR experiments. After the injection of a complementary DNA solution an increase of the sensor response corresponds to the increase of refractive index in the vicinity of LSPR nanoparticles or the SPR sensor surface. After injection of the running buffer the increase of the sensor response stabilize at the level corresponding to the total amount of hybridized DNA probes. For the high concentration of 100 nM, the increase of sensor response levels off which corresponds to the saturation of the sensor surface. For this model system it is possible to assume, that almost all DNA probes are hybridized in the saturation. Comparison of the saturation level obtained with the SPR measurement and the LSPR measurement indicates that the sensor response to a comparable change at the sensor surface would differ only by a small factor. Results presented in Figure 8 indicate virtually identical detection capabilities of the SPR biosensor and the LSPR biosensor also in the sub-nM concentration range.

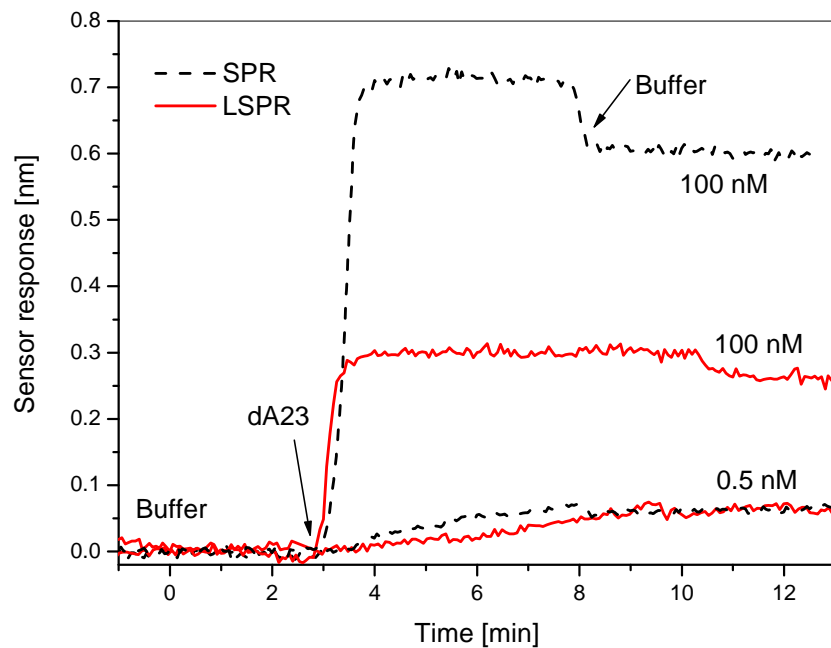


Figure 8 Sensor response to detection DNA hybridization using conventional SPR biosensor (dashed line) and LSPR biosensor utilizing the array of nanorods (solid, red line). Two concentrations (100 nM and 500 pM) of complementary oligonucleotide were used for the comparison.

Preliminary results of biomolecular detection experiments are reported. These experiments were carried out using structures optimized and developed during the visit. Further optimization of the biomolecular detection experiment will be carried out at IPE and the full characterization of the LSPR based biosensor performance is expected to be finished within two months. Publication on the direct comparison of biosensors based on localized surface plasmons and propagating SPR based biosensors is projected within few months.

Summary

The stay at the receiving institution was utilized to merge the know-how and technology available at IPE and KFU and to initiate collaboration on nanoplasmonic biosensors research. KFU nanofabrication facility was used to develop new structures for biosensor application and a new method for investigating nanoparticle arrays was developed. Nanoparticle arrays were optimized for biomolecular detection experiments and a set of nanostructures was fabricated to be used in the development of biomolecular detection assay. The work on the project continues at IPE with the focus on the application. Two publications based on the results obtained during the stay are in preparation and further collaboration on the development of nanoplasmonic biosensors was proposed.

1. J. Homola, "Surface Plasmon Resonance Sensors for Detection of Chemical and Biological Species," *Chem. Rev.* **108**, 462-493 (2008).
2. M. Piliarik, L. Párova, and J. Homola, "High-throughput SPR sensor for food safety," *Biosens. Bioelectron.* **24**, 1399-1404 (2009).
3. M. Piliarik, M. Vala, I. Tichy, and J. Homola, "Compact and low-cost biosensor based on novel approach to spectroscopy of surface plasmons," *Biosens. Bioelectron.* **24**, 3430-3435 (2009).
4. H. Vaisocherova, W. Yang, Z. Zhang, Z. Q. Cao, G. Cheng, M. Piliarik, J. Homola, and S. Y. Jiang, "Ultralow fouling and functionalizable surface chemistry based on a zwitterionic polymer enabling sensitive and specific protein detection in undiluted blood plasma," *Anal. Chem.* **80**, 7894-7901 (2008).
5. F. Fernández, K. Hegnerova, M. Piliarik, F. S. Baeza, J. Homola, and M. P. Marco, "A Label-Free and Portable Multichannel Surface Plasmon Resonance Immunosensor for on site Analysis of Antibiotics in Milk Samples," *Biosens. Bioelectron.*, In print, Available online (2010).
6. D. M. Koller, U. Hohenester, A. Hohenau, H. Ditlbacher, F. Reil, N. Galler, F. Aussenegg, A. Leitner, A. Trugler, and J. R. Krenn, "Superresolution Moiré Mapping of Particle Plasmon Modes," *Phys. Rev. Lett.* **104**, 143901 (2010).
7. S. Chen, M. Svedendahl, M. Kall, L. Gunnarsson, and A. Dmitriev, "Ultrahigh sensitivity made simple: nanoplasmonic label-free biosensing with an extremely low limit-of-detection for bacterial and cancer diagnostics," *Nanotechnology* **20**, - (2009).
8. M. Piliarik, and J. Homola, "Surface plasmon resonance (SPR) sensors: approaching their limits?," *Optics Express* **17**, 16505-16517 (2009).

9. H. Vaisocherova, K. Mrkvova, M. Piliarik, P. Jinoch, M. Steinbachova, and J. Homola, "Surface plasmon resonance biosensor for direct detection of antibody against Epstein-Barr virus," *Biosens. Bioelectron.* **22**, 1020-1026 (2007).
10. H. Vaisocherova, A. Zitova, M. Lachmanova, J. Stepanek, S. Kralikova, R. Liboska, D. Rejman, I. Rosenberg, and J. Homola, "Investigating oligonucleotide hybridization at subnanomolar level by surface plasmon resonance biosensor method," *Biopolymers* **82**, 394-398 (2006).